Remote Sens. **2015**, *7*, 8830-8857; doi:10.3390/rs70708830

OPEN ACCESS

remote sensing

ISSN 2072-4292

www.mdpi.com/journal/remotesensing

Review

The EnMAP Spaceborne Imaging Spectroscopy Mission for Earth Observation

Luis Guanter [1,*], Hermann Kaufmann [1], Karl Segl [1], Saskia Foerster [1], Christian Rogass [1], Sabine Chabrillat [1], Theres Kuester [1], André Hollstein [1], Godela Rossner [2], Christian Chlebek [2], Christoph Straif [2], Sebastian Fischer [2], Stefanie Schrader [2], Tobias Storch [3], Uta Heiden [3], Andreas Mueller [3], Martin Bachmann [3], Helmut Mühle [3], Rupert Müller [3], Martin Habermeyer [3], Andreas Ohndorf [4], Joachim Hill [5], Henning Buddenbaum [5], Patrick Hostert [6], Sebastian van der Linden [6], Pedro J. Leitão [6], Andreas Rabe [6], Roland Doerffer [7], Hajo Krasemann [7], Hongyan Xi [7], Wolfram Mauser [8], Tobias Hank [8], Matthias Locherer [8], Michael Rast [9], Karl Staenz [10] and Bernhard Sang [11]

[1] Helmholtz Center Potsdam, GFZ German Research Center for Geosciences, Remote Sensing Section, Telegrafenberg A17, 14473 Potsdam, Germany; E-Mails: kofmich@gmail.com (H.K.); segl@gfz-potsdam.de (K.S.); foerster@gfz-potsdam.de (S.F.); rogass@gfz-potsdam.de (C.R.); chabri@gfz-potsdam.de (S.C.); theres.kuester@gfz-potsdam.de (T.K.); hollstein@gfz-potsdam.de (A.H.)

[2] Space Administration, German Aerospace Center (DLR), Königswinterer Str. 522-524, 53227 Bonn, Germany; E-Mails: godela.rossner@dlr.de (G.R.); christian.chlebek@dlr.de (C.C.); christoph.straif@dlr.de (C.S.); sebastian.fischer@dlr.de (S.F.); Stefanie.Schrader@dlr.de (S.S.)

[3] Earth Observation Center (EOC), German Aerospace Center (DLR), Münchener Str. 20, 82234 Weßling, Germany; E-Mails: tobias.storch@dlr.de (T.S.); uta.heiden@dlr.de (U.H.); andreas.mueller@dlr.de (A.M.); martin.bachmann@dlr.de (M.B.); helmut.muehle@dlr.de (H.M.); rupert.mueller@dlr.de (R.M.); martin.habermeyer@dlr.de (M.H.)

[4] German Space Operations Center (GSOC), German Aerospace Center (DLR), Münchener Str. 20, 82234 Weßling, Germany; E-Mail: andreas.ohndorf@dlr.de

[5] University of Trier, Environmental Remote Sensing and Geoinformatics, Behringstr. 21, 54286 Trier, Germany; E-Mails: hillj@uni-trier.de (J.H.); buddenbaum@uni-trier.de (H.B.)

[6] Humboldt-Universität zu Berlin, Geography Department, Unter den Linden 6, 10099 Berlin, Germany; E-Mails: patrick.hostert@geo.hu-berlin.de (P.H.); sebastian.linden@geo.hu-berlin.de (S.V.D.L.); p.leitao@geo.hu-berlin.de (P.J.L.); andreas.rabe@geo.hu-berlin.de (A.R.)

[7] Helmholtz-Centre Geesthacht, Institute of Coastal Research, Max Planck-Str. 1, 21502 Geesthacht, Germany; E-Mails: roland.doerffer@hzg.de (R.D.); hajo.krasemann@hzg.de (H.K.); hongyan.xi@hzg.de (H.X.)

[8] Ludwig-Maximilians-University Munich, Department of Geography, Luisenstr. 37, 80333 Munich, Germany; E-Mails: w.mauser@iggf.geo.uni-muenchen.de (W.M.); t.hank@iggf.geo.uni-muenchen.de (T.H.); m.locherer@iggf.geo.uni-muenchen.de (M.L.)
[9] ESA-ESRIN, Via Galileo Galilei, 64, 00044 Frascati Rome, Italy; E-Mail: michael.rast@esa.int
[10] Department of Geography, University of Lethbridge, 4401 University Drive Lethbridge, Lethbridge, AB T1K 3M4, Canada; E-Mail: karl.staenz@uleth.ca
[11] OHB System AG, Perchtinger Str. 5, 81379 Munich, Germany; E-Mail: bernhard.sang@ohb.de

* Author to whom correspondence should be addressed; E-Mail: guanter@gfz-potsdam.de; Tel.: +49-331-288-1190; Fax: +49-331-288-1192.

Academic Editors: Clement Atzberger and Prasad S. Thenkabail

Received: 30 April 2015 / Accepted: 6 July 2015 / Published: 13 July 2015

Abstract: Imaging spectroscopy, also known as hyperspectral remote sensing, is based on the characterization of Earth surface materials and processes through spectrally-resolved measurements of the light interacting with matter. The potential of imaging spectroscopy for Earth remote sensing has been demonstrated since the 1980s. However, most of the developments and applications in imaging spectroscopy have largely relied on airborne spectrometers, as the amount and quality of space-based imaging spectroscopy data remain relatively low to date. The upcoming Environmental Mapping and Analysis Program (EnMAP) German imaging spectroscopy mission is intended to fill this gap. An overview of the main characteristics and current status of the mission is provided in this contribution. The core payload of EnMAP consists of a dual-spectrometer instrument measuring in the optical spectral range between 420 and 2450 nm with a spectral sampling distance varying between 5 and 12 nm and a reference signal-to-noise ratio of 400:1 in the visible and near-infrared and 180:1 in the shortwave-infrared parts of the spectrum. EnMAP images will cover a 30 km-wide area in the across-track direction with a ground sampling distance of 30 m. An across-track tilted observation capability will enable a target revisit time of up to four days at the Equator and better at high latitudes. EnMAP will contribute to the development and exploitation of spaceborne imaging spectroscopy applications by making high-quality data freely available to scientific users worldwide.

Keywords: EnMAP; imaging spectroscopy; hyperspectral remote sensing; environmental applications; Earth observation

---

1. Introduction

Optical imaging spectroscopy or hyperspectral remote sensing for Earth observation relies on the use of spectrometers for the measurement of the solar radiation reflected by Earth system components in contiguous spectral channels [1,2]. The reconstruction of atmospheric and surface absorption features from spectroscopic measurements enables the identification and quantification of land, water and atmosphere constituents with characteristic spectral signatures, which makes imaging spectrometers suited for a wide range of Earth observation applications. The potential of airborne and spaceborne imaging spectrometers has long been exploited to monitor the Earth's surface and atmosphere and to provide valuable information for the better understanding of a large number of environmental processes (e.g., [3,4]). Those applications include, for example, vegetation monitoring and ecology (e.g., [5–11]), geology and soils (e.g., [12–17]), coastal and inland waters (e.g., [18–21]), mapping of snow properties [22,23] and archaeological prospection [24,25].

Most of the developments in imaging spectroscopy in the last few decades have been based on airborne spectrometers covering the visible to near-infrared (VNIR) and, often, shortwave-infrared (SWIR) spectral ranges (roughly, 400–1000 nm and 1000–2500 nm, respectively). In particular, the Airborne Visible/Infrared Imaging Spectrometer (AVIRIS) [26,27], designed and operated by the NASA Jet Propulsion Laboratory in California, has been used since the late 1980s in a large number of imaging spectroscopy experiments and field campaigns. Other airborne imaging spectrometers widely used in the last few years are HyMAP [28], the Compact Airborne Spectrographic Imager (CASI) [29] and the Airborne Prism Experiment (APEX) [30,31].

Unfortunately, the recognized potential of imaging spectroscopy is currently not counterbalanced by an equivalent availability of spaceborne imaging spectroscopy data. Two technology demonstration missions, Hyperion onboard NASA's Earth Observing-1 (EO-1) spacecraft [32] and the Compact High Resolution Imaging Spectrometer (CHRIS) on ESA's Proba-1 microsatellite [33], have been the main providers of space-based hyperspectral data over the last few decades. Even though both missions have largely exceeded their planned one-year lifetime, they are still very valuable sources of publicly-available spaceborne hyperspectral data. Hyperion, launched in November 2000, is a grating spectrometer measuring in the 400–2500 nm spectral range with a 10-nm spectral sampling distance (SSD), a 30-m ground sampling distance (GSD) and a 7.7-km swath width. CHRIS, in turn, is a VNIR prism-based spectrometer launched onboard Proba-1 in October 2001. In its hyperspectral mode, the CHRIS/Proba system acquires $14 \times 14\,\mathrm{km}^2$ scenes in the 400–1000-nm spectral range with an SSD of about 10 nm and a GSD of 34 m. Coexisting with Hyperion and CHRIS/Proba, the Medium Resolution Imaging Spectrometer (MERIS) [34] onboard ENVISAT operated during 2003–2012. Although only 15 (binned) spectral channels are made available to standard users, MERIS was conceived of as an imaging spectrometer measuring in the 400–900-nm spectral range with 1.25-nm spectral sampling. Lately, the Hyperspectral Imager for the Coastal Ocean (HICO) [35], developed by NASA and the U.S. Office of Naval Research, has provided imaging spectroscopy data in the VNIR over coastal regions since its deployment on the International Space Station in September 2009 until the end of the mission in March 2015. Furthermore, the Indian Hyperspectral Imager (HySI) onboard the Indian Micro Satellite-1

(IMS-1) [36] and the Chinese HJ-1A [37] provide VNIR hyperspectral data, although with only limited access for international scientific users.

Overall, those experimental systems are playing an important role as precursors for operational spaceborne imaging spectroscopy missions, but the amount and quality of data are unfortunately insufficient for a wide range of potential application fields of imaging spectroscopy. The Environmental Mapping and Analysis Program (EnMAP) German imaging spectroscopy mission [38–41] is intended to cover this gap in spaceborne imaging spectroscopy for Earth observation. EnMAP is a joint response of German Earth observation research institutions, value-added resellers and space industry to the increasing demand for accurate, quantitative information about the status and evolution of terrestrial ecosystems. After a competitive and successfully accomplished definition phase, EnMAP was approved by the German Aerospace Agency (DLR in the German name) in the beginning of 2006 and is currently in the construction phase with launch planned for mid-2018.

EnMAP is expected to become a key system in the field of spaceborne imaging spectroscopy in potential co-existence with other comparable and complementary missions, such as the Japanese Hyperspectral Imager Suite (HISUI) [42], the Italian PRISMA (Hyperspectral Precursor of the Application Mission) [43], the USA's Hyperspectral Infrared Imager (HyspIRI) [44], the French HYPXIM [45] and the Italian-Israeli SHALOM (Spaceborne Hyperspectral Applicative Land and Ocean Mission). Even though no coordination between different missions for the optimization of acquisitions is foreseen, imaging spectroscopy users will benefit from the larger diversity of data sources. In addition, the Sentinel-2 [46] and Landsat-8 [47] multispectral systems will also co-exist with EnMAP and share a similar spectral coverage, spatial sampling and focus on land applications. Those two multispectral missions hold the prospect of becoming ideal partners for EnMAP in the development of synergetic applications exploiting the wide spatial coverage and short revisit time of Sentinel-2 and Landsat-8 together with EnMAP's continuous spectral sampling of the VNIR and SWIR regions.

This contribution presents a review of the EnMAP mission and ongoing preparatory activities. An overview of the mission requirements and internal organization is provided in Section 2. The main modules of the EnMAP space and ground segments are described in Sections 3 and 4. Ongoing activities towards the development of critical technical and scientific mission components are discussed in Sections 5 and 6. Finally, a short summary of the main aspects covered throughout the text is provided in Section 7.

2. Mission Overview

2.1. Mission and Instrument Requirements

EnMAP relies on a prism-based dual-spectrometer instrument design to cover the 420–2450-nm spectral range. An artistic representation of an EnMAP overpass depicting the field-of-view of the VNIR and SWIR spectrometers and other acquisition details is displayed in Figure 1. The VNIR spectrometer covers the 420–1000-nm spectral range with an SSD between 5.5 and 7.5 nm, whereas the SWIR spectrometer covers 900–2450 nm with an SSD between 8.5 and 11.5 nm. Spectral resolution is required to be about 1.2 larger than the sampling distance. Threshold requirements for the signal-to-noise

ratio (SNR) at the reference radiance level, defined by 30% surface albedo, 30° Sun zenith angle (SZA), 0.5 km above sea level and 21 km atmospheric visibility, are 400:1 and 180:1 for the VNIR and SWIR ranges, respectively, with a 14-bit radiometric resolution. The required radiometric calibration accuracy is 5%, and the spectral calibration uncertainty is 0.5 nm in the VNIR and 1 nm in the SWIR. Spatial sampling is defined by a GSD of 30 m, a swath width of 30 km and a length in multiples of 30 km up to 1000 km per orbit and 5000 km per day (limitations mostly posed by onboard memory and power consumption constraints). The selected orbit is Sun-synchronous, with a local time of 11:00 for the descending node. An off-nadir pointing capability of up to 30° enables a revisit time of four days at the Equator and better at higher latitudes. The expected mission lifetime is five years. A summary of selected mission and instrument parameters is presented in Table 1.

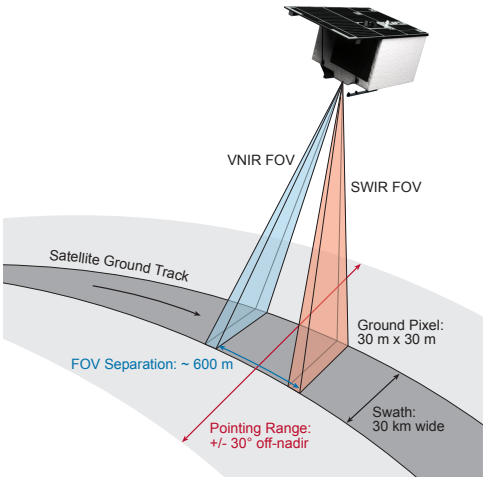

Figure 1. Representation of an EnMAP overpass featuring the dual-spectrometer instrument concept. The field-of-views (FOVs) of the visible near-infrared (VNIR) and shortwave infrared (SWIR) spectrometers are represented in blue and red, respectively.

Table 1. Selected EnMAP mission and instrument specifications. The reference radiance level for the definition of signal-to-noise ratio (SNR) figures is 30% surface albedo, 30° Sun zenith angle, 0.5 km above sea level and 21 km atmospheric visibility. VZA stands for view zenith angle, VNIR for visible near-infrared and SWIR for shortwave infrared.

Mission Requirements	
Spectral range	420–2450 nm
Ground sampling distance	30 m
Swath width	30 km
Swath length	up to 1000 km/orbit
Coverage	Global in near-nadir mode (VZA $\leq$5°)
Orbit	Sun-synchronous,11:00 local time descending node
Daily coverage	5000 km

Table 1. *Cont.*

Mission Requirements	
Target revisit time	4 days with 30°across-track pointing
Pointing accuracy (knowledge)	500 (100) m at sea level
Instrument Requirements	
Imaging principle	Push-broom-prism
Spectral range	VNIR: 420–1000 nm/SWIR: 900–2450 nm
Mean spectral sampling distance	VNIR: 6.5 nm/SWIR: 10 nm
Spectral oversampling	1.2
SNR at reference radiance	>400:1 at 495 nm/>180:1 at 2200 nm
Spectral calibration accuracy	VNIR: 0.5 nm/SWIR: 1 nm
Spectral stability	0.5 nm
Radiometric calibration accuracy	<5%
Radiometric stability	<2.5%
Radiometric resolution	14 bit, dual gain in VNIR
Sensitivity to polarization	<5%
Spectral smile/keystone effect	<20% of a pixel
Co-registration VNIR-SWIR	<20% of a pixel

2.2. Mission Organization

The EnMAP project is being executed by a series of institutions and governing bodies with specific tasks. These can be listed as follows (http://www.enmap.org/?q=organization):

- Scientific principal investigator at the GFZ (German acronym for German Research Center for Geosciences) in Potsdam, Germany: the principal investigator is responsible for the definition of the scientific objectives and requirements of the EnMAP Mission, the development of the EnMAP science plan, the advice to project management on trade-offs between technical and scientific issues during mission implementation and the conception and coordination of the validation of data products.
- The EnMAP Science Advisory Group (EnSAG) is headed by the scientific principal investigator and composed of international imaging spectroscopy experts. The EnSAG provides advice to the DLR Space Administration on the mission's scientific objectives, maintains the EnMAP Science Plan document, monitors the agreement between the scientific objectives and the EnMAP program execution, provides recommendations for complementary activities and raises awareness of EnMAP data in the scientific community.
- Project management is led by the DLR Space Administration in Bonn-Oberkassel, Germany. It is responsible for the overall project management, including the implementation and operation of the ground segment and for contracting the industrial consortium for the development of the space segment.

- The EnMAP ground segment is led by the Earth Observation Center (EOC) at DLR in Oberpfaffenhofen, Germany. It comprises: (i) the mission operation system, controlling and commanding platform and instrument; (ii) the payload ground system, responsible for data reception, data processing and archiving and disseminating data products to users; and (iii) the processor and calibration/quality control system developing the processing system capable of generating calibrated data products at several processing levels, calibrating the sensor and performing data product quality control.
- The EnMAP space segment is led by OHB System AG. Space segment activities include building the satellite bus, designing and manufacturing the payload, the integration and testing of the entire satellite, the procurement of the flight opportunity, including launch support and preparation, and the launch itself.

The different components of the EnMAP space and ground segments are briefly presented in the next sections.

3. Space Segment

3.1. Instrument

3.1.1. Dual Spectrometer Instrument Concept

The push-broom type instrument features two prism-based spectrometers for the VNIR and the SWIR spectral ranges coupled to a field splitter slit assembly, which carries two separate slits for in-field separation and a micro-mirror to redirect the SWIR field into the SWIR spectrometer. A schematic view of the instrument design is presented in Figure 2. The slit is located at the image plane of a near diffraction-limited three mirror anastigmatic telescope with an across-track field of view of $\pm 1.3°$. Radiation enters the system through a calibration device, which allows switching between Earth view, full-aperture Sun diffuser calibration and launch protection modes. A baffling system ensures good out-of-field stray light performance. The spectrometer optics with unit magnification are derived from an Offner relay imaging concept and employ curved Fery-type prisms in dual pass configuration as dispersion elements. This configuration allows for high throughput, low polarization sensitivity and low smile and keystone distortions. Two 2D focal planes acquire images at a frame rate of 230 Hz with 14-bit resolution. The SWIR system features a mercury-cadmium-telluride (MCT)-type detector coupled to an integrated read-out circuit, which is operated at 150 K by the use of a pulse tube cryocooler. The VNIR system consists of a highly functionally-integrated back-illuminated complementary metal-oxide-semiconductor (CMOS) imager with on-chip analog-to-digital converters (ADCs). The optical system, a mixed material system with aluminum mirrors and two types of glass, is housed in an aluminum structure with stringent heater control to achieve a high stability of critical performance parameters, such as spectral stability and co-registration. The instrument line-of-sight is coupled to the attitude control system by a high stability sensor assembly structure to achieve good system pointing knowledge. Further details on the instrument concept can be found in [40,48].

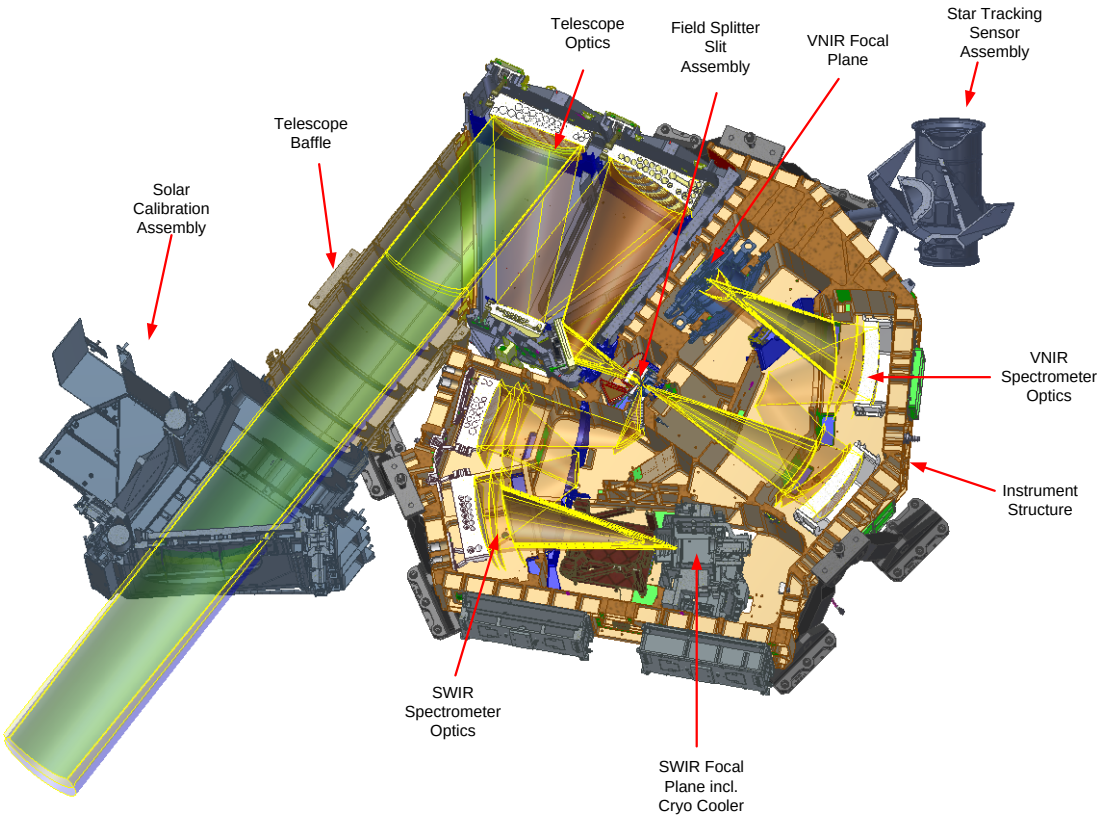

Figure 2. Schematic view of the main components of the EnMAP double-spectrometer instrument concept.

3.1.2. Spectral and Radiometric Performance

Detailed knowledge of the instrument performance based on a consolidated instrument model are already available for some key spectral and radiometric parameters of EnMAP. The spectral coverage and resolution of the two spectrometers is depicted in Figure 3. A typical top-of-atmosphere (TOA) radiance spectrum from a dry sand surface was simulated with the MODTRAN5 atmospheric radiative transfer code [49] at a spectral resolution of 0.5 nm and convolved with the EnMAP spectral response. The SSD is plotted as a function of wavelength in the lower panel. Mean SSD is about 6.5 nm in the VNIR and 10 nm in the SWIR. The spectral resolution is requested to be 1.2 larger than the SSD to avoid spectral artifacts due to signal undersampling. The variation of the SSD with wavelength, caused by the dispersion properties of the glasses, is characteristic for prism-based spectrometers [48].

The uniformity of an imaging spectrometer represents the degree of variability of the spectral and spatial responses in the two dimensions of the detector array [50]. In particular, the smile effect describes the variation of the center wavelength of a given spectral channel along the spatial (across-track) direction. The keystone effect is the counterpart of smile in the spatial domain. This is the variation of a pixel's spatial position with wavelength. Spectrally- and spatially-uniform datasets are required to fully exploit the information in hyperspectral measurements [4]. Even though EnMAP's optical design based on curved prisms is intended to minimize smile and keystone distortions, *a priori* knowledge of the spectral and spatial uniformity of a spectrometer response is needed for proper data processing and interpretation. The expected magnitude of smile and keystone in the VNIR and SWIR spectrometers

as a function of spectral and spatial position in the VNIR and SWIR focal plane arrays is displayed in Figure 4. Characteristic spectral "smile" and "frown" (inverse smile) patterns can be observed along the across-track direction of the SWIR spectrometer at, e.g., 1000- and 2400-nm wavelength positions, respectively. Peak values of smile are about −0.5 nm (∼5% of a spectral pixel) at the long wavelength edges of the two spectrometers, which is to be compared with the up to 4-nm variation in spectral channel position at 760 nm for Hyperion [51]. Keystone is generally below 3% of a spatial pixel for the EnMAP VNIR spectrometer and almost negligible in the SWIR spectrometer. These numbers for smile and keystone largely improve upon the $< 20\%$ mission requirement (see Table 1).

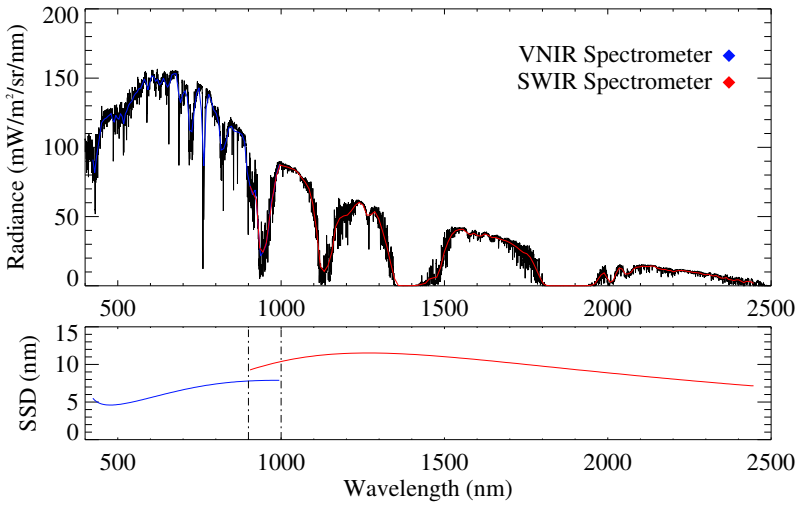

Figure 3. Illustration of EnMAP spectral characteristics. (**Top**) Simulated top-of-atmosphere radiance spectrum for a dry sand surface convolved by the EnMAP spectral response. (**Bottom**) Spectral sampling distance (SSD) as a function of wavelength.

Figure 4. Expected spectral smile (**left**) and keystone (**right**) effects for the two EnMAP spectrometers as a function of spectral and spatial positions in the VNIR and SWIR focal plane arrays (**top** and **bottom**, respectively). The mission requirements of smile and keystone $<20\%$ are largely fulfilled thanks to the curved prism disperser approach adopted for the spectrometers' optical system.

The radiometric sensitivity of EnMAP is defined by SNR specifications of 400:1 at 495 nm and 180:1 at 2200 nm for a given reference radiance level and by a 14-bit radiometric resolution (see Table 1).

The existing instrument model can be used to estimate the actual spectral SNR as a function of at-sensor radiance. Examples for four land cover types representing different application fields of EnMAP are displayed in Figure 5. For the sake of a simpler interpretation, the incoming at-sensor radiance used for the SNR simulation is expressed in terms of spectral surface reflectance at SZA = 45°. Because of EnMAP's prism-based design, multiplicative shot-noise is the main contribution to the measurement noise at medium and high radiance levels, causing the spectral SNR to roughly scale with the square root of the incoming at-sensor radiance. This explains that the SNR in the examples in Figure 5 is highest for the brighter kaolinite spectrum and lowest for the water spectrum and that there is a drop in SNR at the spectral regions in which incoming radiance decreases because of atmospheric absorptions (see the TOA radiance spectrum in Figure 3).

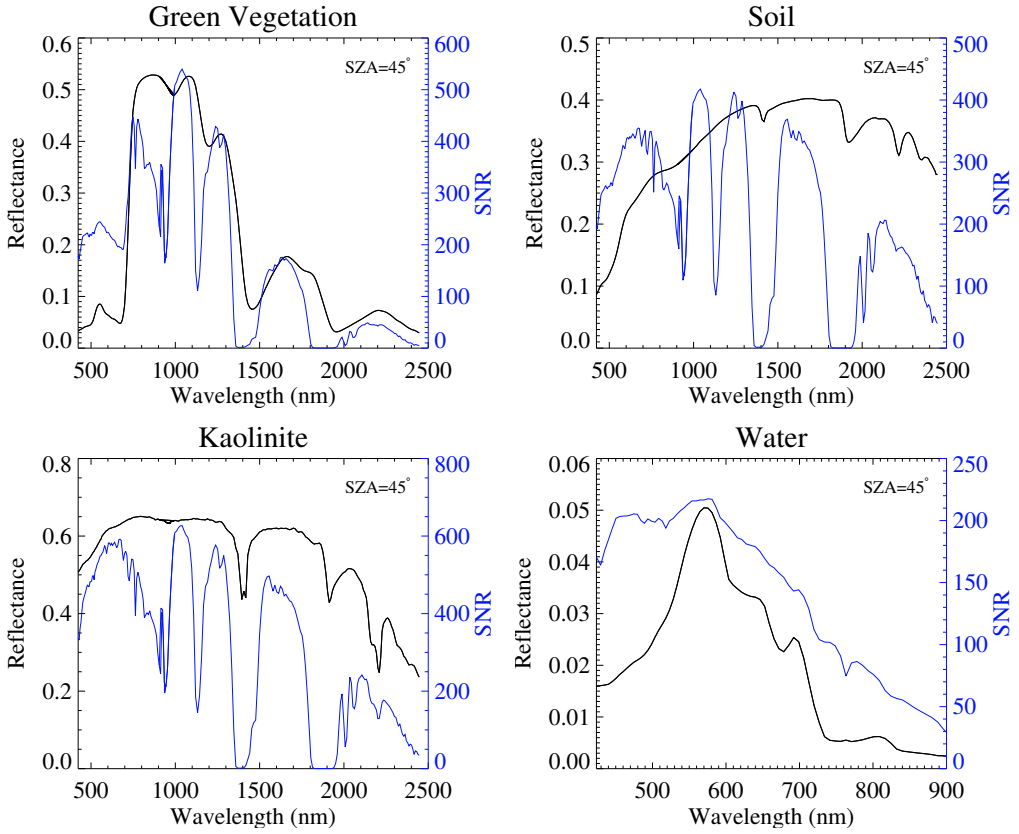

Figure 5. Simulated spectral signal-to-noise ratio (SNR) for incoming radiance levels corresponding to a Sun zenith angle (SZA) of 45° and surface reflectance spectra representing different EnMAP application fields.

Regarding the EnMAP 14-bit radiometric resolution, the instrument electronics in the VNIR are designed to automatically switch the radiometric gain between high and low as a function of the incoming radiance, which is encoded in the last one of the 14 bits. This allows covering the entire dynamic range of the instrument with a linear relationship between the input radiance levels and the digital numbers registered at the detector and, at the same time, provides a sufficient radiometric sensitivity at the lowest radiance levels covered by the high gain mode. The red-green-blue (RGB) composites in Figure 6 show the effects of this dual radiometric gain system. The transitions from pinkish to yellowish patches over

bare soil surfaces in the RGB image derived from digital number data correspond to areas in which the radiometric gain has been switched. This effect is corrected during radiometric calibration so that the effect of the two gains is no longer visible in radiometrically-calibrated radiance data.

Figure 6. Red-green-blue composites from a simulated EnMAP dataset over Barrax (Spain) illustrating the conversion from digital numbers (**left**) to radiometrically-calibrated radiance data (**right**). The switch between high and low radiometric gain modes is visible in the digital number image as yellowish and pinkish patches.

3.2. On-Board Calibration Facilities

During EnMAP operations, a series of spectral and radiometric characterization activities will be carried out taking advantage of on-board calibration facilities. Detector linearity calibration and suspicious pixel mapping will be performed using light-emitting diodes (LEDs) mounted in front of the detectors in conjunction with the ability of the focal planes to control integration time in a wide parameter range. Spectral calibration on-orbit will be performed using the spectral mode of the on-board calibration device where a rare earth-doped diffuser is used to illuminate the spectrometer entrance slits with a radiance spectrum with well-defined and stable spectral structures. The shift in spectral parameters up to second order can be retrieved by comparing the predicted system performance with on-board measurements. The calibration system based on an Ulbricht integrating sphere will be used in its radiometric mode to create repeatable and smooth spectral radiance for assessing the radiometric properties of the spectrometers. This facility allows the monitoring of the instrument at small time intervals in order to confirm the validity of the radiometric calibration. Primary radiometric calibration will be achieved by the use of a full-aperture diffuser system with a well-characterized bidirectional reflectance distribution function. A mechanism introduces the diffuser into the optical beam and opens the diffuser protection hatch to allow for direct Sun illumination, thereby generating a well-known spectral radiance at the entrance pupil of the instrument. Finally, the shutter calibration mechanism allows the blocking of all light from entering the spectrometers in order to perform frequent dark signal calibrations. The same mechanism switches the optical path from the telescope view (Earth observation

and Sun calibration) to the Ulbricht integrating sphere (spectral calibration and radiometric validation). A schematic view of on-board calibration devices is displayed in Figure 7.

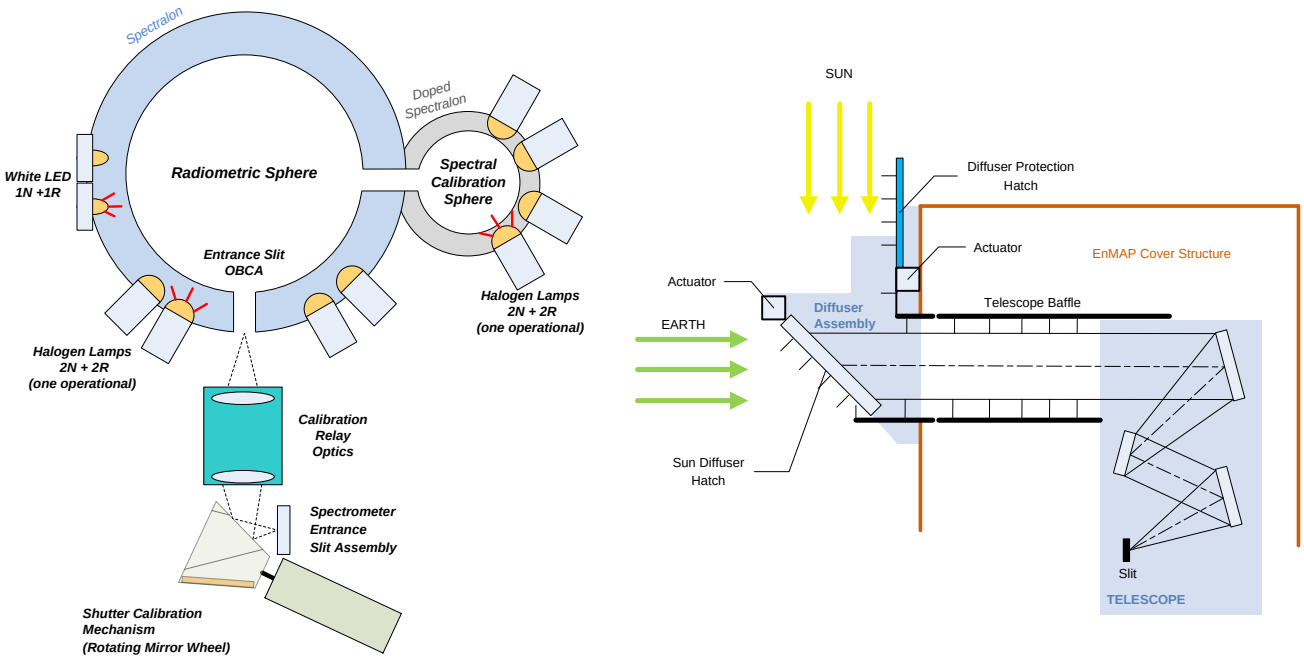

Figure 7. On-board calibration units of the EnMAP instrument. For spectral and relative radiometric calibration, the Ulbricht integrating sphere (**left**) provides a homogeneous source of illumination for the spectrometer entrance slits via coupling optics and a mechanism that introduces a mirror into the telescope beam. Absolute radiometric calibration is performed by using the Sun to illuminate the entrance pupil of the telescope via a Spectralon full-aperture diffuser (**right**).

3.3. Platform and Launcher

The EnMAP platform is a reuse of an existing design of OHB System AG space heritage. It comprises accurate orbit and attitude control and a high rate data processing chain and features three-axis stabilization and a mass memory system for data storage. The input image data stream of 866 Mbit/s is stored in five memory banks configured such that "graceful degradation" is tolerated, resulting in 512 Gbit of end-of-life memory capacity. Lossless data compression based on the Consultative Committee for Space Data Systems (CCSDS) Standard 122 is performed individually for each spectral band. This JPEG2000-based compression achieves an average compression ratio of 1.6 with a dedicated field programmable gate array (FPGA). The mass memory output is routed through a CCSDS coding unit directly to the 320-Mbit/s X-band downlink system. More information about the satellite platform can be found in [40].

The satellite dimensions are compatible with the Indian Polar Satellite Launch Vehicle (PSLV). Launch is expected to take place from Sriharikota, India.

4. Ground Segment

The setup and operation of the EnMAP ground segment is under the responsibility of the Earth Observation Center (EOC) and the German Space Operations Center (GSOC) at the DLR [52]. The ground segment completed its design phase by successfully passing the critical design review in 2010 and is now in production phase.

The ground segment is organized into 15 systems covering all relevant aspects to assure successful mission operations. This comprises controlling and commanding the satellite using multi-mission infrastructures, as well as data reception, hyperspectral data processing (including calibration), data archiving, data dissemination and provision of web-interfaces to the international user community. Two major topics of particular interest for the users are addressed next. These are the handling of image acquisitions based on user requests and the generation of standardized products.

4.1. Acquisition Plan and Operations

EnMAP is able to acquire 5000 km along-track per day with 30 km across-track based on the acquisition requests of users that are specified via an online interface [53]. A user request consists of:

- Center of the geographical area of interest between 80° north and 80° south.
- Length of the geographical area of interest as a multiple of 30 km and up to 1000 km.
- Definition of the allowed maximum across-track satellite tilt angle (between 5° and 30°).
- Time period when the acquisition shall be executed.

Acquisitions are planned for the descending orbit. Only observations with SZA $< 60°$ are considered in order to guarantee acceptable illumination conditions. Table 2 illustrates the resulting revisit capabilities in descending orbits for six different latitudes and two values of the maximum across track tilt angle. All areas of interest in Table 2 can be observed with a tilt angle lower than 3.1°.

Table 2. Maximum and mean revisit time (RT) in descending orbits for six different latitudes, represented by areas of interest, and two maximum across track tilt angles (TAs).

Latitude	Area of Interest	Max RT with TA $< 30°$	Mean RT with TA $< 30°$	Max RT with TA $< 5°$	Mean RT with TA $< 5°$
0°	Libreville, Gabon	4 days	3.4 days	27 days	19.9 days
15°	Niger, Niger	4 days	3.2 days	27 days	18.2 days
30°	Tripoli, Libya	4 days	2.8 days	27 days	16.3 days
45°	Munich, Germany	4 days	2.3 days	23 days	11.5 days
60°	Oslo, Norway	3 days	1.5 days	19 days	8.1 days
75°	Longyearbyen, Norway	1 days	0.7 days	7 days	3.7 days

Although EnMAP is based on an open data policy and every type of user is in principle entitled to download data and request acquisitions, there will be different user categories to set acquisition priorities. In short, Category 1 users (Cat. 1) will be scientific users who have submitted a research proposal

describing how they plan to use the data. Scientific proposals will be evaluated and rated by the EnSAG and potential external reviewers. In turn, Category 2 users (Cat. 2) will be non-registered international public or private entities. The priorities for requests to be considered are, in decreasing order: internal (e.g., calibration), emergency Cat. 2 (e.g., international charter on space and major disasters), Cat. 1 (with high rated scientific proposal), Cat. 1 (with low rated scientific proposal), non-emergency Cat. 2, internal (low, e.g., to fill up or extend requests). Requests of the first two priorities are scheduled regardless of their success concerning cloud probabilities or quota. Thus, especially requests of the last four priorities shall take the revisit times into account for setting the time period appropriately to increase the probability that the scheduling fulfills the request. Of course, this depends on the specific area of interest and further requirements on the observation. Whether a specific user request is scheduled for execution is based on:

- Satellite resources (e.g., available data storage, scheduled data downlinks and orbit maneuvers for orbit maintenance or collision avoidance).
- Quota, e.g., 80% for all Cat. 1 users (registered) in the first year to 60% in the fifth year, where internal users are not considered.
- Cloud probabilities (e.g., historical and predicted cloud coverages).

The users shall place a request at least 25 h before the intended execution to ensure its uplink, because an S-band contact (4 Kbit/s uplink, 32 Kbit/s downlink) via the Weilheim, Germany, multi-mission ground station is scheduled at least every 12 h and planning of the conflict-free sequence of events takes one hour.

The image data, as well as orbit and attitude data are transmitted during several X-band contacts (320 Mbit/s downlink) per day via the Neustrelitz, Germany, multi-mission ground station. All data are available for further processing to data products at most 24 h after acquisition.

4.2. Data Products

The EnMAP ground segment will distribute a series of data products with different processing levels as detailed in Table 3. In the first steps of the default processing chain, the acquired image files are complemented by auxiliary channel files (one for VNIR and one for SWIR) stored during imaging. These files are combined with refined orbit and attitude measurements, as well as sensor-specific spectral, radiometric and geometric calibration tables (see Figure 8, dotted lines) to generate internal Level 0 products, which are long-term archived. Next, standardized Earth observation products at several processing levels are created, termed Level 1B, Level 1C and Level 2A. Quality information is annotated at the end of each level.

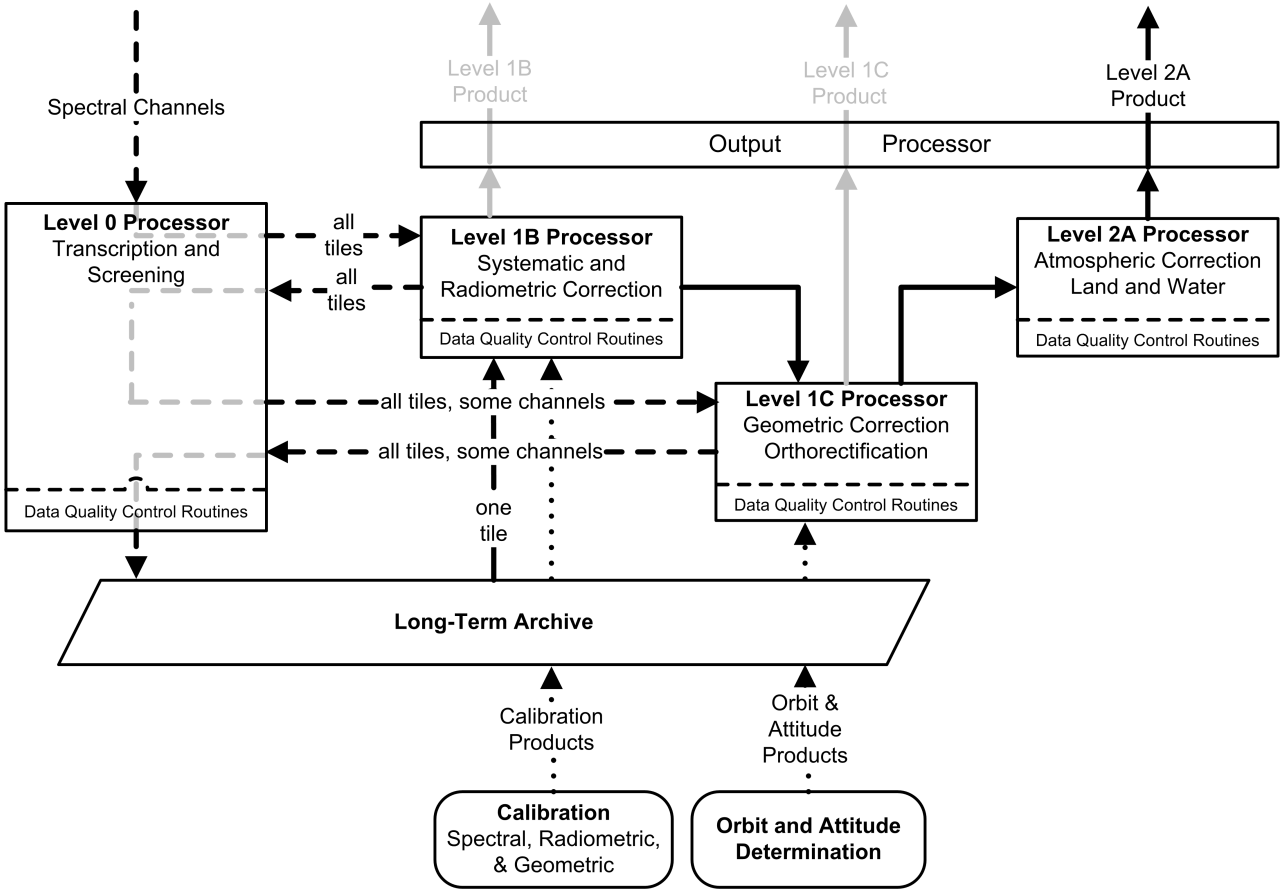

Figure 8. Scheme of the processing chain for the generation of data products at the EnMAP ground segment.

Level 0 processing (see Figure 8, dashed lines) comprises the following steps:

1. Decompress image channel files, if files are (loss-less) compressed.
2. Check status, e.g., that values and standard deviations are in specified range of dark current measurements and determine dark signal information for each pixel.
3. Perform Level 1B processing for all channels.
4. Improve geometric accuracy by:
   (a) Coarsely registering (by affine transformation) the mono-chromatic VNIR channel closest in wavelength to the one of the reference image (RI) to be extracted from the Sentinel-2 global RI database.
   (b) Performing hierarchical intensity-based image matching with the RI, resulting in homologous points.
   (c) After a highly selective blunder detection and removal, three-dimensional ground control points are generated with a digital elevation model (DEM), which is intended to be extracted from the ASTER global DEM database.
   (d) Instrument mounting angles and attitude products are improved, and quality information is included.
   (e) Performing Level 1C processing for a subset of channels.

5. Performing pixel classification, e.g., land-water and cloud-haze-cirrus-clear, and determining the visibility map (based on dark pixels for land) allowing the estimation of the aerosol optical thickness.
6. Generating quick looks and quality data with 8 bits.
7. Long-term archiving of the Level 0 product for all tiles.

Level 1B processing comprises the following steps to correct for systematic effects and convert the image data into physical at-sensor radiance values:

1. Flag dead pixels based on calibration tables, saturated (hot) and no-response (cold) pixels based on image data, as well as the first and last 12 pixels of each frame, which are dark current measurements used for quality control.
2. Correction for non-linearities, dark signal and response non-uniformity based on look-up tables.
3. Perform gain matching for the VNIR detector, since the low or high gain is automatically selected.
4. Correction for stray light for the spectral and spatial direction based on correction matrices.
5. Perform spectral referencing, through which center wavelength and the full width at half maximum are assigned to spectral channels, and radiometric referencing in order to convert 32-bit floating point values to 16-bit integers for storage.
6. Final data screening for striping and other remaining artifacts, generation of data quality flags and metadata.

Level 1C processing converts Level 1B products into map-accurate forms. The map projection and resampling technique can be chosen by the user. Finally, Level 2A processing converts Level 1C products to surface reflectances, where separate algorithms for land and water applications are employed. The correction mode can be chosen by the user, namely land-water, land, water. Atmospheric correction involves the generation of sun glitter maps for water surfaces by identification of specular reflections, the detection (and correction) of haze and cirrus, the estimation of aerosol optical thickness and columnar water vapor and the retrieval of surface reflectance after adjacency correction. All information related to the data quality derived during the entire processing is documented in the metadata and within per-pixel data quality flags [54].

Table 3. Definition of EnMAP data products.

Product	Definition
Level 0	Time-tagged instrument raw data with auxiliary information (internal)
Level 1B	Radiometrically-corrected, spectrally- and geometrically-characterized radiance
Level 1C	Orthorectified Level 1B
Level 2A	Atmospherically-corrected Level 1C

Typically, Level 0 products are contained in the archive allowing searching and ordering by users via an online interface at most 24 h after completion of the corresponding downlink. Afterwards, the processing and delivery of Level 2A products (see Figure 8, solid lines), including geometric and atmospheric corrections, is typically conducted in at most 8 h. As the format for not long-term

archived products, the user can choose an image format of band-sequential, band-interleaved-by-line, and band-interleaved-by-pixel encoding (BSQ, BIL and BIP, respectively), JPEG2000 and GeoTIFF, whereas the metadata format is always Extensible Markup Language (XML). A report in portable document format (PDF) is appended to the product.

5. Development of the EnMAP Science Plan

One of the key advantages of imaging spectroscopy is its adaptability to a wide range of research fields and environmental applications. These include, among others, terrestrial and aquatic ecosystems, natural resource management, hazards and risks and atmospheric research. The reader is referred to existing reviews on imaging spectroscopy (e.g., [3,4]) for a comprehensive overview of those topics. Particular aspects of those general topics are currently being developed in the framework of the EnMAP preparatory phase by the EnSAG [55], as well as in other activities, such as PhD projects funded by the EnMAP science program. Specific research tasks currently under development by the EnSAG towards the consolidation of the EnMAP science plan comprise the following:

- Agriculture: EnMAP will open new perspectives for remote sensing in agriculture. This central branch of the economy is challenged by supplying enough food and bio-materials for a growing and wealthier global population and by making agricultural production sustainable. Increasing resource use efficiency, namely water, energy, fertilizers and soil, by turning farm management into an information and knowledge business will allow both. "Smart farming" eventually aims at using crop-growth models and remote sensing data to most efficiently manage each location on each field on the globe by choosing the right crop and the right time for sowing, for applying the right amount of fertilizer and pesticides and for harvesting [56]. Today empirical relations translate multi-spectral image data into crop parameters, which enter crop-growth models. This procedure is region and crop specific, expensive and inflexible and hampers the introduction of remote sensing in smart farming. Therefore, research within the EnMAP preparatory program focuses on developing new ways to derive crop parameters, like leaf-area index, biomass, chlorophyll and nitrogen content, directly from hyperspectral EnMAP simulator data using first order physical and physiological principles. The approach uses a tightly-coupled system of crop growth and crop radiative transfer models to derive spatio-temporal fields of crop parameters through iterative ensemble analysis [57]. A model for the realistic simulation of the hyperspectral and multiangular reflectance response of virtual 3D cereal canopies has also been implemented in the framework of EnMAP [58].
- Forest: Forests provide innumerable ecological, societal and climatological benefits, but have also been exposed to increasing pressure from environmental changes, such as global warming and human population growth. The most important processes occurring in forests (e.g., carbon exchange, photosynthesis and respiration, evapotranspiration, nutrient cycling) are difficult to measure. Ecosystem models have been developed to simulate the fluxes of matter and energy and to increase the understanding of scale- and time-dependency in these processes. However, remote sensing-derived leaf and canopy variables are needed to constrain such models, and it has been suggested that hyperspectral imaging systems allow more detailed and accurate retrieval of

these properties [59]. Forest ecosystems are particularly vulnerable to drought and temperature extremes. Climate-driven forest die-off from drought and heat stress has already occurred around the world and is expected to further increase with climate change. Hyperspectral imaging from space has a great potential to become one of the most important information sources for identifying critical, drought-affected forest sites, particularly in synergy with higher spatial resolution data acquired at increased repetition rates (e.g., Sentinel-2 and -3). Research priorities are focusing on testing efficient spectral indicators, alongside the refinement of algorithms for forest-type mapping, the detection of structural changes and gradients in forest ecosystems (e.g., [60]) and forward and inverse radiative transfer modeling. Controlled laboratory and field experiments will continue to provide important backup information for algorithmic optimization.

- Natural ecosystems and ecosystem transitions: EnMAP specifically creates opportunities for monitoring spatially-heterogeneous landscapes and environmental gradients [61]. Through monitoring and analysis of complex natural ecosystem processes, it is possible to deepen the understanding of anthropogenic impacts and to contribute to global mitigation programs, such as the United Nation's Reducing Emissions from Deforestation and Forest Degradation (REDD) or the Convention on Biological Diversity. By offering global and multitemporal coverage at Landsat- and Sentinel-2-like spatial resolution, EnMAP will provide a powerful spectroscopy tool, which is valuable for detailed ecosystem characterization and answering complex ecological questions, such as monitoring natural vegetation and vegetation dynamics or understanding the spatial patterns of biodiversity and biotic communities [62,63]. EnMAP has also a great potential for better understanding environmental gradients resulting from anthropogenic disturbances, such as the urban to rural land cover gradient. Research conducted in and around Berlin, Germany, using simulated EnMAP data has further improved the vegetation impervious soil framework in this context [64].
- Geology: The timely availability of raw materials is critical for manufacturing sectors. The demand for fast and spatially-extensive geological exploration is ever growing together with the necessity to monitor residual mining areas. EnMAP enables short-term geological exploration of minerals and metals and long-term mine waste monitoring using the EnGeoMAP software [16,65]. Sharp, distinctive absorptions of rare earth element oxides, such as neodymium oxide, partially modulated by broad iron absorptions, can be explored using high-pass and absorption feature techniques and semi-quantified to map local enrichment and its spatio-temporal distribution for mine waste monitoring. The full wavelength range of EnMAP is required for a spaceborne characterization of hydrothermal alteration zones and gossans using spectroscopic mapping of mineral distribution patterns to indicate copper-, gold-, silver- and iron-enriched ores through distinct absorption features of minerals that are characteristic for these deposit types.
- Soil science: EnMAP offers new opportunities for retrieving accurate, up-to-date, quantitative soil information required for mapping the status of the world's soils and for monitoring soil degradation processes, such as erosion, loss of organic matter, contamination, salinization and compaction. Based on previous expertise in soil spectroscopy at the field and airborne scale, soil activities in the EnMAP preparatory program are focusing on: (i) development of algorithms for semi-quantitative soil mapping of key soil parameters (such as organic carbon, soil moisture, clay, carbonate and

iron content) and extension of current methods for fully-quantitative soil mapping [17], including the development of the EnMAP Soil Mapper (EnSoMAP) processor; (ii) demonstration of the potential of imaging spectroscopy for fractional ground cover and soil degradation stages mapping at different spatial scales; and (iii) demonstration of the potential of the EnMAP satellite for digital soil mapping [66].

- Coastal and inland waters: Existing sensors and algorithms for water applications are designed mainly for open ocean waters. Coastal and inland waters are characterized by highly-complex constituent composition and need consequential complex optical analysis. Furthermore, the spatial resolution of current multiband sensors is not sufficient for smaller lakes or rivers. EnMAP opens new possibilities, whose potential for water quality assessment are studied in the EnMAP preparatory program. This includes research on optical models for high absorbing coastal waters [67] and on hyperspectral absorption of dissolved salts [68], as well as the influence of particle composition and particle size to the mass-specific absorption of light. The differentiation of phytoplankton groups using derivative analysis of hyperspectral data is also being investigated.
- Urban areas: Since the turn of the century, more people are thought to live in cities than in rural areas. Airborne and spaceborne remote sensing approaches are frequently used to provide spatial information to characterize, monitor and manage urban areas. Imaging spectroscopy started to be used for urban studies mainly based on airborne sensor data in the 1990s and has subsequently led to detailed and automated urban surface material mapping using material specific spectral characteristics [69]. Recent analysis of simulated EnMAP data showed its potential for more detailed and accurate maps on urban fraction cover than, for example, at Landsat spectral resolution [64]. However, due to the lack of spaceborne imaging spectrometers, the potential for urban studies has not yet been fully explored. Still, the relative coarse geometric resolution of sensors like EnMAP is not sufficient to resolve most of the small-scale urban objects, such as buildings and streets. Thus, combining EnMAP spectral information with other high spatial resolution information, such as multispectral satellite data (e.g., Sentinel-2, WorldView), digital surface models and spectral libraries of surface materials, is thought to be useful [70]. Spectral mixture analysis approaches will be developed accounting for the high spectral heterogeneity of urban areas. The derived surface material abundance maps can then be used to generate maps of surface imperviousness, detect hazardous materials or as input to urban micro-climate models. EnMAP's lifetime, spatial coverage and revisit time will allow repeatedly observing large cities on the globe and the continuous reporting of changes.

6. Other Ongoing Preparatory Activities

6.1. End-to-End Scene Simulations

The design of future Earth imaging systems, the optimization of fundamental instrument parameters and the development and evaluation of data pre-processing algorithms require an accurate end-to-end simulation of the entire image generation and processing chain. For this purpose, the EnMAP end-to-end simulation software EeteS has been developed [71–73]. The sequential processing chain starts with

the EnMAP image simulator that consists of four independent parts, namely the atmospheric, spatial, spectral and radiometric modules. This forward simulator is coupled to a backward simulation branch consisting of calibration modules (non-linearity, dark current and absolute radiometric calibration) and a series of pre-processing modules (radiometric calibration, co-registration, atmospheric correction and orthorectification), forming the complete end-to-end simulation tool. The implemented modules allow flexible customization of a wide range of simulation input parameters. EeteS is capable of simulating EnMAP-like data products that also serve as a test bench for other pre-launch developments, such as new algorithms for the improved scientific-exploitation of future EnMAP data. Sample datasets generated with the EeteS are shown in Figure 9. The EeteS is offered on-demand to scientific users for the simulation of acquisitions over additional sites.

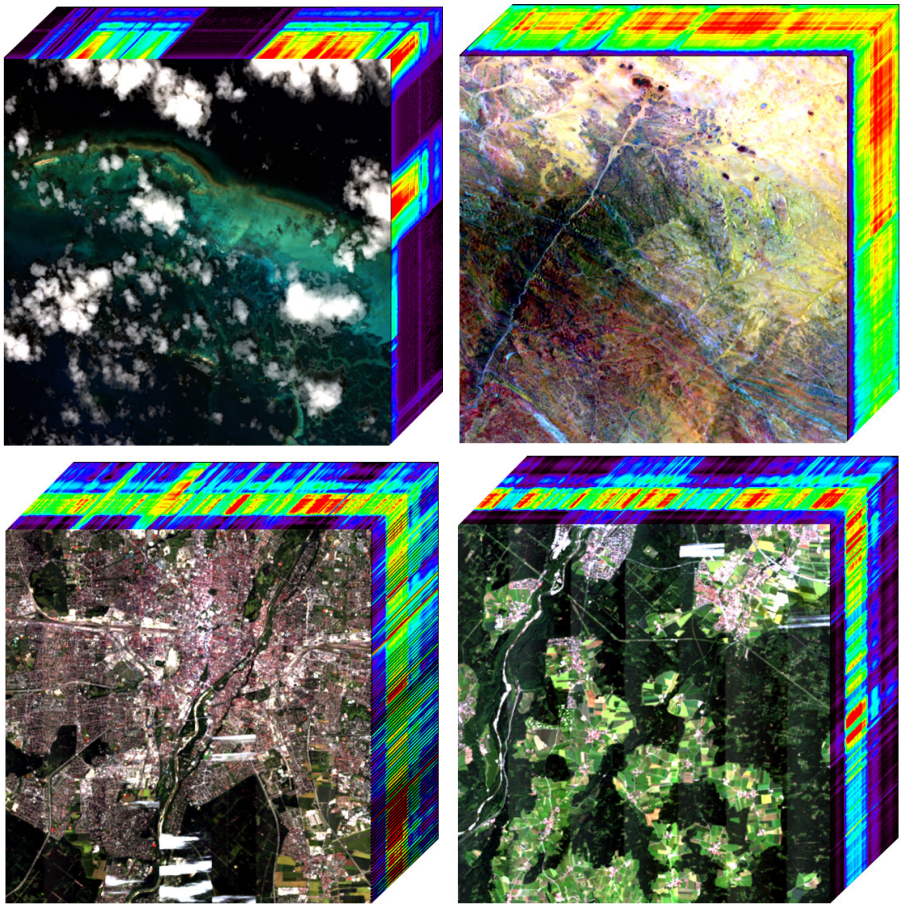

Figure 9. Scenes generated from simulated EnMAP scenes corresponding to different data applications. The hypercubes represent red-green-blue composites from a geological site in Namibia (**top left**), French Frigate Shoals in the Northwestern Hawaiian Islands (**top right**) and two acquisitions around the Munich area in Germany (**bottom**).

6.2. Post-Launch Calibration and Validation Plan

The EnMAP post-launch calibration plan is based on the monitoring and processing of on-board measured instrument parameters. It is currently being developed by the ground segment at DLR-EOC, which is also implementing methods for an operational, quantitative and qualitative product quality

assessment. Complementing and supporting the calibration plan, GFZ is developing a strategy for vicarious validation of EnMAP user products. The general aim of this strategy is to complement ground segment data quality assessments with quantities that are not considered in the monitoring and calibration plan, as well as to provide independent means to assess product quality parameters. Accurate and well-calibrated ground-based measurements of surface and atmospheric parameters at selected sites will be used to estimate representative error figures for EnMAP data. In addition, image-based data quality checks, spectral calibration analysis and the assessment of geometric calibration will be addressed within this strategy.

6.3. Preparatory Field Campaigns

A number of pre-flight campaigns, including airborne acquisitions and extensive *in situ* measurements, are being deployed in the framework of the EnMAP preparatory phase. The main purpose of these campaigns is to support the development of scientific applications for EnMAP by evaluating the potential performance for the retrieval of key environmental parameters, exploiting synergies with multispectral systems, as well as developing and validating image processing algorithms. In addition, the acquired datasets collected in a wide range of environments are being used for testing data pre-processing and calibration/validation methods and are input for EnMAP end-to-end scene simulations. The data are made freely available to the scientific community under a Creative Commons License (CC BY-SA 4.0). The EnMAP pre-flight campaigns started in 2008 and are ongoing. An overview of all available datasets is provided through a specifically-developed data portal (http://www.enmap.org/?q=flightbeta).

6.4. EnMAP-Box

Given the special requirements of the work with imaging spectroscopy data, a software toolbox is developed as part of the EnMAP mission preparation. The two overarching aims for the development of the so-called EnMAP-Box are (i) extending the EnMAP data user community beyond that of airborne imaging spectroscopy data and (ii) providing free access to the most recent methods for hyperspectral data processing. In order to achieve these aims, the EnMAP-Box is provided as an open source program code with a comprehensive application programming interface to allow the easy standardized integration of algorithmic developments from the imaging spectroscopy community. The latest version of the EnMAP-Box is freely available at http://www.enmap.org/?q=enmapbox; it contains, among others, user-friendly implementations of support vector classification and regression, random forest classification and regression, as well as several applications for pre-processing (atmospheric correction, spatial resampling, *etc*.) and analysis of EnMAP-like data. For more details, see the contribution by van der Linden *et al*. [74].

7. Conclusions

EnMAP is a spaceborne imaging spectroscopy mission developed by a consortium of German Earth observation institutions with the main purpose of filling the current gap in global, high-quality and operational hyperspectral data. An overview of the mission and its current status has been provided in this

contribution. EnMAP will measure in the VNIR and SWIR spectral regions of the solar spectrum with a spectral sampling of 5–10 nm, a ground sampling distance of 30 m and an image swath width of 30 km. EnMAP hyperspectral measurements will enable the monitoring of a wide span of Earth materials and environmental processes. Data products from different pre-processing levels (from calibrated at-sensor radiance to orthorectified surface reflectance data) will be delivered to scientific users under an open data policy. A series of core research topics within the EnMAP science plan, such as agriculture, forestry, water, ecosystem science, soils and geology and urban environments, is currently being addressed through a series of EnMAP-specific research programs. Other on-going preparatory activities include the simulation of EnMAP-like datasets over different environments for testing data pre-processing and application-based algorithms, the consolidation of the calibration-validation plan and the implementation of a software toolbox for the processing and exploitation of EnMAP data.

Acknowledgments

EnMAP is funded under the DLR Space Administration with resources from the German Federal Ministry of Economic Affairs and Energy and contributions from DLR, GFZ and OHB System AG.

Author Contributions

The development of the manuscript concept, the collection of the materials for the different sections and the overall coordination of the work was performed by Luis Guanter and Hermann Kaufmann. Luis Guanter also wrote the abstract, introduction and conclusions. Karl Segl provided text about end-to-end simulations, Saskia Foerster and Theres Kuester about preparatory field campaigns, André Hollstein about post-launch calibration and validation plan, Tobias Storch, Uta Heiden, Andreas Mueller, Martin Bachmann, Helmut Mühle, Rupert Müller, Martin Habermeyer and Andreas Ohndorf about ground segment operations and data products (Section 4), Bernhard Sang about the instrument concept and on-board calibration facilities, and Sebastian van der Linden and Andreas Rabe about the EnMAP-Box. Text on the different application fields of the EnMAP Science Plan (Section 5) was provided by Christian Rogass (geology), Sabine Chabrillat (soils), Joachim Hill and Henning Buddenbaum (forest), Patrick Hostert and Pedro J. Leitão (natural ecosystems), Roland Doerffer, Hajo Krasemann and Hongyan Xi (water), and Wolfram Mauser, Tobias Hank, Matthias Locherer (agriculture). Finally, Godela Rossner, Christian Chlebek, Christoph Straif, Sebastian Fischer, Stefanie Schrader, Michael Rast and Karl Staenz provided general aspects of the mission organization. All the authors have reviewed and commented on the subsequent versions of the manuscript.

Conflicts of Interest

The authors declare no conflict of interest.

References

1. Goetz, A.F.H.; Vane, G.; Salomon, J.E.; Rock, B.N. Imaging spectroscopy for earth remote sensing. *Science* **1985**, *228*, 1147–1153.

2. Vane, G.; Goetz, A.F.H. Terrestrial imaging spectroscopy for earth remote sensing. *Remote Sens. Environ.* **1988**, *24*, 1–29.
3. Schaepman, M.E.; Ustin, S.L.; Plaza, A.J.; Painter, T.H.; Verrelst, J.; Liang, S. Earth system science related imaging spectroscopy-An assessment. *Remote Sens. Environ.* **2009**, *113*, S123–S137.
4. Green, R.O. Lessons and key results from 30 years of imaging spectroscopy. *Proc. SPIE* **2014**, *9222*, doi:10.1117/12.2062426.
5. Gamon, J.; Peñuelas, J.P.; Field, C. A narrow-waveband spectral index that tracks diurnal changes in photosynthetic efficiency. *Remote Sens. Environ.* **1992**, *41*, 35–44.
6. Sims, D.A.; Gamon, J.A. Estimation of vegetation water content and photosynthetic tissue area from spectral reflectance: A comparison of indices based on liquid water and chlorophyll absorption features. *Remote Sens. Environ.* **2003**, *84*, 526–537.
7. Ustin, S.L.; Roberts, D.A.; Gamon, J.A.; Asner, G.P.; Green, R.O. Using imaging spectroscopy to study ecosystem processes and properties. *BioScience* **2004**, *54*, 523–534.
8. Asner, G.P. Biophysical and biochemical sources of variability in canopy reflectance. *Remote Sens. Environ.* **1998**, *64*, 234–253.
9. Roberts, D.; Gardner, M.; Church, R.; Ustin, S.; Scheer, G.; Green, R. Mapping chaparral in the santa monica mountains using multiple endmember spectral mixture models. *Remote Sens. Environ.* **1998**, *65*, 267–279.
10. Asner, G.P.; Nepstad, D.; Cardinot, G.; Ray, D. Drought stress and carbon uptake in an Amazon forest measured with spaceborne imaging spectroscopy. *Proc. Natl. Acad. Sci. USA* **2004**, *101*, 6039–6044.
11. Ustin, S.L.; Gitelson, A.; Jacquemoud, S.; Schaepman, M.; Asner, G.P.; Gamon, J.A.; Zarco-Tejada, P. Retrieval of foliar information about plant pigment systems from high resolution spectroscopy. *Remote Sens. Environ.* **2009**, *113*, S67–S77.
12. Kruse, F.; Lefkoff, A.; Dietz, J. Expert system-based mineral mapping in northern death valley, California/Nevada, using the Airborne Visible/Infrared Imaging Spectrometer (AVIRIS). *Remote Sens. Environ.* **1993**, *44*, 309–336.
13. Clark, R.N.; Swayze, G.A.; Livo, K.E.; Kokaly, R.F.; Sutley, S.J.; Dalton, J.B.; McDougal, R.R.; Gent, C.A. Imaging spectroscopy: Earth and planetary remote sensing with the USGS Tetracorder and expert systems. *J. Geophys. Res. Planets* **2003**, *108*, doi:10.1029/2002JE001847.
14. Ben-Dor, E.; Chabrillat, S.; Demattê, J.; Taylor, G.; Hill, J.; Whiting, M.; Sommer, S. Using Imaging Spectroscopy to study soil properties. *Remote Sens. Environ.* **2009**, *113*, S38–S55.
15. Van der Meer, F.D.; van der Werff, H.M.; van Ruitenbeek, F.J.; Hecker, C.A.; Bakker, W.H.; Noomen, M.F.; van der Meijde, M.; Carranza, E.J.M.; de Smeth, J.B.; Woldai, T. Multi- and hyperspectral geologic remote sensing: A review. *Int. J. Appl. Earth Obs. Geoinf.* **2012**, *14*, 112–128.
16. Mielke, C.; Boesche, N.K.; Rogass, C.; Kaufmann, H.; Gauert, C.; de Wit, M. Spacebornee mine waste mineralogy monitoring in South Africa, applications for modern push-broom Missions: Hyperion/OLI and EnMAP/Sentinel-2. *Remote Sens.* **2014**, *6*, 6790–6816.
17. Chabrillat, S.; Ben-Dor, E.; Rossel, R.A.V.; Demattê, J.A. Quantitative soil spectroscopy. *Appl. Environ. Soil Sci.* **2013**, *2013*, 616578.

18. Brando, V.; Dekker, A. Satellite hyperspectral remote sensing for estimating estuarine and coastal water quality. *IEEE Trans. Geosci. Remote Sens.* **2003**, *41*, 1378–1387.
19. Moses, W.J.; Gitelson, A.A.; Perk, R.L.; Gurlin, D.; Rundquist, D.C.; Leavitt, B.C.; Barrow, T.M.; Brakhage, P. Estimation of chlorophyll-a concentration in turbid productive waters using airborne hyperspectral data. *Water Res.* **2012**, *46*, 993–1004.
20. Hunter, P.D.; Tyler, A.N.; Carvalho, L.; Codd, G.A.; Maberly, S.C. Hyperspectral remote sensing of cyanobacterial pigments as indicators for cell populations and toxins in eutrophic lakes. *Remote Sens. Environ.* **2010**, *114*, 2705–2718.
21. Giardino, C.; Brando, V.E.; Dekker, A.G.; Strömbeck, N.; Candiani, G. Assessment of water quality in Lake Garda (Italy) using Hyperion. *Remote Sens. Environ.* **2007**, *109*, 183–195.
22. Painter, T.H.; Dozier, J.; Roberts, D.A.; Davis, R.E.; Green, R.O. Retrieval of subpixel snow-covered area and grain size from imaging spectrometer data. *Remote Sens. Environ.* **2003**, *85*, 64–77.
23. Dozier, J.; Green, R.O.; Nolin, A.W.; Painter, T.H. Interpretation of snow properties from imaging spectrometry. *Remote Sens. Environ.* **2009**, *113*, S25–S37.
24. Atzberger, C.; Wess, M.; Doneus, M.; Verhoeven, G. ARCTIS-A MATLAB© toolbox for archaeological imaging spectroscopy. *Remote Sens.* **2014**, *6*, 8617–8638.
25. Cavalli, R.M.; Colosi, F.; Palombo, A.; Pignatti, S.; Poscolieri, M. Remote hyperspectral imagery as a support to archaeological prospection. *J. Cult. Herit.* **2007**, *8*, 272–283.
26. Vane, G.; Green, R.O.; Chrien, T.G.; Enmark, H.T.; Hansen, E.G.; Porter, W.M. The airborne visible/infrared imaging spectrometer (AVIRIS). *Remote Sens. Environ.* **1993**, *44*, 127–143.
27. Green, R.O.; Eastwood, M.; Sarture, C.; Chrien, T.; Aronsson, M.; Chippendale, B.; Faust, J.; Pavri, B.; Chovit, C.; Solis, M.; *et al*. Imaging spectroscopy and the airborne visible/infrared imaging spectrometer (AVIRIS). *Remote Sens. Environ.* **1998**, *65*, 227–248.
28. Cocks, T.; Jenssen, R.; Stewart, A.; Wilson, I.; Shields, T. The HyMap airborne hyperspectral sensor: The system, calibration and performance. In Proceedings of the First EARSeL Workshop on Imaging Spectroscopy, Zurich, Switzerland, 6–8 October 1998; pp. 37–42.
29. Itres Research Ltd. Available online: http://www.itres.com/cgi-bin/products.cgi?sensor=11 (accessed 20 April 2015).
30. Itten, K.I.; Dell'Endice, F.; Hueni, A.; Kneubuehler, M.; Schlaeper, D.; Odermatt, D.; Seidel, F.; Huber, S.; Schopfer, J.; Kellenberger, T.; *et al*. APEX—The hyperspectral ESA airborne prism experiment. *Sensors* **2008**, *8*, 6235–6259.
31. Schaepman, M.E.; Jehle, M.; Hueni, A.; D'Odorico, P.; Damm, A.; Weyerrnann, J.; Schneider, F.D.; Laurent, V.; Popp, C.; Seidel, F.C.; *et al*. Advanced radiometry measurements and Earth science applications with the Airborne Prism Experiment (APEX). *Remote Sens. Environ.* **2015**, *158*, 207–219.
32. Ungar, S.G.; Pearlman, J.S.; Mendenhall, J.A.; Reuter, D. Overview of the earth observing one (EO-1) mission. *IEEE Trans. Geosci. Remote Sens.* **2003**, *41*, 1149–1159.
33. Barnsley, M.J.; Settle, J.J.; Cutter, M.; Lobb, D.; Teston, F. The PROBA/CHRIS mission: A low-cost smallsat for hyperspectral, multi-angle, observations of the Earth surface and atmosphere. *IEEE Trans. Geosci. Remote Sens.* **2004**, *42*, 1512–1520.

34. Rast, M.; Bézy, J.L.; Bruzzi, S. The ESA Medium Resolution Imaging Spectrometer MERIS–a review of the instrument and its mission. *Int. J. Remote Sens.* **1999**, *20*, 1681–1702.
35. Lucke, R.L.; Corson, M.; McGlothlin, N.R.; Butcher, S.D.; Wood, D.L.; Korwan, D.R.; Li, R.R.; Snyder, W.A.; Davis, C.O.; Chen, D.T. Hyperspectral imager for the coastal ocean: Instrument description and first images. *Appl. Opt.* **2011**, *50*, 1501–1516.
36. Kumar, A.; Saha, A.; Dadhwal, V.K. Some issues related with sub-pixel classification using HYSI data from IMS-1 satellite. *J. Indian Soc. Remote Sens.* **2010**, *38*, 203–210.
37. Zhao, X.; Xiao, Z.; Kang, Q.; Li, Q.; Fang, L. Overview of the fourier transform Hyperspectral Imager (HSI) boarded on HJ-1A satellite. In Proceedings of the 2010 IEEE International Geoscience and Remote Sensing Symposium (IGARSS), Honolulu, HI, USA, 25–30 July 2010; pp. 4272–4274.
38. Kaufmann, H.; Segl, K.; Guanter, L.; Hofer, S.; Foerster, K.P.; Stuffler, T.; Mueller, A.; Richter, R.; Bach, H.; Hostert, P.; *et al*. Environmental Mapping and Analysis Program (EnMAP)—Recent advances and status. In Proceedings of the International Geoscience and Remote Sensing Symposium (IGARSS), Boston, MA, USA, 7–11 July 2008.
39. Stuffler, T.; Kaufmann, C.; Hofer, S.; Foerster, K.; Schreier, G.; Mueller, A.; Eckardt, A.; Bach, H.; Penné, B.; Benz, U.; *et al*. The EnMAP hyperspectral imager—An advanced optical payload for future applications in Earth observation programmes. *Acta Astronaut.* **2007**, *61*, 115–120.
40. Qian, S.E. (Ed.) *Optical Payloads for Space Missions*; Wiley: Hoboken, NJ, USA, 2015; p. 948.
41. EnMAP. Available online: http://www.enmap.org/ (accessed on 20 April 2015).
42. Iwasaki, A.; Ohgi, N.; Tanii, J.; Kawashima, T.; Inada, H. Hyperspectral Imager Suite (HISUI)—Japanese hyper-multi spectral radiometer. In Proceedings of the 2011 IEEE International Geoscience and Remote Sensing Symposium (IGARSS), Vancouver, BC, USA, 24–29 July 2011; pp. 1025–1028.
43. Stefano, P.; Angelo, P.; Simone, P.; Filomena, R.; Federico, S.; Tiziana, S.; Umberto, A.; Vincenzo, C.; Acito, N.; Marco, D.; *et al*. The PRISMA hyperspectral mission: Science activities and opportunities for agriculture and land monitoring. In Proceedings of the 2013 IEEE International Geoscience and Remote Sensing Symposium (IGARSS), Melbourne, Australia, 21–26 July 2013; pp. 4558–4561.
44. Green, R.; Asner, G.; Ungar, S.; Knox, R. NASA mission to measure global plant physiology and functional types. In Proceedings of the 2008 IEEE Aerospace Conference, Big Sky, MT, USA, 1–8 March 2008; pp. 1–7.
45. Michel, S.; Gamet, P.; Lefevre-Fonollosa, M.J. HYPXIM—A hyperspectral satellite defined for science, security and defence users. In Proceedings of the 2011 3rd Workshop on Hyperspectral Image and Signal Processing: Evolution in Remote Sensing (WHISPERS), Lisbon, Portugal, 6–9 June 2011; pp. 1–4.
46. Drusch, M.; Bello, U.D.; Carlier, S.; Colin, O.; Fernandez, V.; Gascon, F.; Hoersch, B.; Isola, C.; Laberinti, P.; Martimort, P.; *et al*. Sentinel-2: ESA's optical high-resolution mission for GMES operational services. *Remote Sens. Environ.* **2012**, *120*, 25–36.

47. Roy, D.; Wulder, M.; Loveland, T.; C.E.W.; Allen, R.; Anderson, M.; Helder, D.; Irons, J.; Johnson, D.; Kennedy, R.; *et al*. Landsat-8: Science and product vision for terrestrial global change research. *Remote Sens. Environ.* **2014**, *145*, 154–172.
48. Sang, B.; Schubert, J.; Kaiser, S.; Mogulsky, V.; Neumann, C.; Förster, K.P.; Hofer, S.; Stuffler, T.; Kaufmann, H.; Müller, A.; *et al*. The EnMAP hyperspectral imaging spectrometer: Instrument concept, calibration, and technologies. *Proc. SPIE* **2008**, *7086*, doi:10.1117/12.794870.
49. Berk, A.; Anderson, G.P.; Acharya, P.K.; Bernstein, L.S.; Muratov, L.; Lee, J.; Fox, M.; Adler-Golden, S.M.; Chetwynd, J.H., Jr.; Hoke, M.L.; *et al*. MODTRAN5: 2006 update. *Proc. SPIE* **2006**, *6233*, doi:10.1117/12.665077.
50. Nieke, J.; Schlapfer, D.; Dell'Endice, F.; Brazile, J.; Itten, K. Uniformity of imaging spectrometry data products. *IEEE Trans. Geosci. Remote Sens.* **2008**, *46*, 3326–3336.
51. Gao, B.C.; Montes, M.J.; Davis, C.O. Refinement of wavelength calibrations of hyperspectral imaging data using a spectrum-matching technique. *Remote Sens. Environ.* **2004**, *90*, 424–433.
52. Storch, T.; Habermeyer, M.; Eberle, S.; Mühle, H.; Müller, R. Towards a critical design of an operational ground segment for an earth observation mission. *J. Appl. Remote Sens.* **2013**, *7*, doi:10.1117/1.JRS.7.073581.
53. Heiden, U.; Gredel, J.; Pinnel, N.; MuÌĹhle, H.; Pengler, I.; Reissig, K.; Dietrich, D.; Heinen, T.; Storch, T.; Eberle, S.; *et al*. The user interface of the EnMAP satellite mission. In Proceedings of the 2010 IEEE International Geoscience and Remote Sensing Symposium (IGARSS), Honolulu, HI, USA, 25–30 July 2010; pp. 4268–4271.
54. Müller, R.; Bachmann, M.; Chlebek, C.; Krawcyk, H.; de Miguel, A.; Palubinskas, G.; Richter, R.; Schneider, M.; Schwind, P.; Storch, T.; *et al*. The EnMAP hyperspectral satellite mission: An overview and selected concepts. In Proceedings of the Third Annual Hyperspectral Imaging Conference Istituto Nazionale di Geofisica e Vulcanologia, Rome, Italy, 15–16 May 2012.
55. Kaufmann, H.; Hill, J.; Hostert, P.; Krasemann, H.; Mauser, W.; Muller, A. *Science Plan of the Environmental Mapping and Analysis Program (EnMAP)*; Technical Report; Deutsches GeoForschungsZentrum GFZ Potsdam: Potsdam, Germany, 2012.
56. Mauser, W.; Bach, H.; Hank, T.; Zabel, F.; Putzenlechner, B. How spectroscopy from space will support world agriculture. In Proceedings of the IEEE International Geoscience and Remote Sensing Symposium (IGARSS), Munich, Germany, 22–27 July 2012; pp. 7321–7324.
57. Migdall, S.; Klug, P.; Denis, A.; Bach, H. The additional value of hyperspectral data for smart farming. In Proceedings of the IEEE International Geoscience and Remote Sensing Symposium (IGARSS), Munich, Germany, 22–27 July 2012; pp. 7329–7332.
58. Kuester, T.; Spengler, D.; Barczi, J.F.; Segl, K.; Hostert, P.; Kaufmann, H. Simulation of multitemporal and hyperspectral vegetation canopy bidirectional reflectance using detailed virtual 3-D canopy models. *IEEE Trans. Geosci. Remote Sens.* **2014**, *52*, 2096–2108.
59. Ollinger, S.; Smith, M.L. Net primary production and canopy nitrogen in a temperate forest landscape: An analysis using imaging spectroscopy, modeling and field data. *Ecosystems* **2005**, *8*, 760–778.

60. Buddenbaum, H.; Seeling, S.; Hill, J. Fusion of full-waveform LiDAR and imaging spectroscopy remote sensing data for the characterization of forest stands. *Int. J. Remote Sens.* **2013**, *34*, 4511–4524.
61. Leitão, P. J.; Schwieder, M.; Suess, S.; Okujeni, A.; Galvão, L.S. van der Linden, S.; Hostert, P. Monitoring natural ecosystem and ecological gradients: Perspectives with EnMAP. *Remote Sens.* **2015**, under review.
62. Schwieder, M.; Leitão, P.J.; Suess, S.; Senf, C.; Hostert, P. Estimating fractional shrub cover using simulated EnMAP data: A comparison of three machine learning regression techniques. *Remote Sens.* **2014**, *6*, 3427–3445.
63. Leitão, P.J.; Schwieder, M.; Suess, S.; Catry, I.; Milton, E.J.; Moreira, F.; Osborne, P.E.; Pinto, M.J.; van der Linden, S.; Hostert, P. Mapping beta diversity from space: Sparse Generalized Dissimilarity Modelling (SGDM) for analysing high-dimensional data. *Methods Ecol. Evol.* **2015**, doi:10.1111/2041-210X.12378.
64. Okujeni, A.; van der Linden, S.; Hostert, P. Extending the vegetation-impervious-soil model using simulated EnMAP data and machine learning. *Remote Sens. Environ.* **2015**, *158*, 69–80.
65. Rogass, C.; Segl, K.; Mielke, C.; Fuchs, Y. EnGeoMAP-A geological mapping tool applied to the EnMAP mission. *EARSeL EProc.* **2013**, *12*, 94–100.
66. Chabrillat, S.; Foerster, S.; Steinberg, A.; Segl, K. Prediction of common surface soil properties using airborne and simulated EnMAP hyperspectral images: Impact of soil algorithm and sensor characteristic. In Proceedings of the 2014 IEEE International Geoscience and Remote Sensing Symposium (IGARSS), Quebec City, QC, Canada, 13–18 July 2014; pp. 2914–2917.
67. Örek, H.; Doerffer, R.; Röttgers, R.; Boersma, M.; Wiltshire, K.H. Contribution to a bio-optical model for remote sensing of Lena River water. *Biogeosciences* **2013**, *10*, 7081–7094.
68. Röttgers, R.; McKee, D.; Utschig, C. Temperature and salinity correction coefficients for light absorption by water in the visible to infrared spectral region. *Opt. Express* **2014**, *22*, 25093–25108.
69. Heiden, U.; Heldens, W.; Roessner, S.; Segl, K.; Esch, T.; Mueller, A. Urban structure type characterization using hyperspectral remote sensing and height information. *Landsc. Urban Plan.* **2012**, *105*, 361–375.
70. Heldens, W.; Heiden, U.; Esch, T.; Stein, E.; Mueller, A. Can the future EnMAP mission contribute to urban applications? A literature survey. *Remote Sens.* **2011**, *3*, 1817–1846.
71. Guanter, L.; Segl, K.; Kaufmann, H. Simulation of optical remote-sensing scenes with application to the EnMAP hyperspectral mission. *IEEE Trans. Geosci. Remote Sens.* **2009**, *47*, 2340–2351.
72. Segl, K.; Guanter, L.; Kaufmann, H.; Schubert, J.; Kaiser, S.; Sang, B.; Hofer, S. Simulation of spatial sensor characteristics in the context of the EnMAP hyperspectral mission. *IEEE Trans. Geosci. Remote Sens.* **2010**, *48*, 3046–3054.
73. Segl, K.; Guanter, L.; Rogass, C.; Kuester, T.; Roessner, S.; Kaufmann, H.; Sang, B.; Mogulsky, V.; Hofer, S. EeteS—The EnMAP end-to-end simulation tool. *IEEE J. Sel. Top. Appl. Earth Obs. Remote Sens.* **2012**, *5*, 522–530.

74. Van der Linden, S.; Rabe, A.; Held, M.; Jakimow, B.; Leitão, P.J.; Okujeni, A.; Suess, S.; Hostert, P. The EnMAP-Box—A toolbox and application programming interface for EnMAP data processing. *Remote Sens.* **2015**, under review.